Original Article

Comparison of chest computed tomography in Turbo FLASH mode with conventional mode for coronary artery disease screening: radiation dose, image quality, and calcium scoring performance

Ying-Lan Shu[#]^, Han Yu[#]^, Da-Jing Guo^, Ya-Ping Huang^, Wen-Li Jiang^, Yin-Deng Luo[*]^, Jie Xu[*]^

Department of Radiology, The Second Affiliated Hospital of Chongqing Medical University, Chongqing, China

Contributions: (I) Conception and design: YL Shu, H Yu, DJ Guo, YD Luo, J Xu; (II) Administrative support: DJ Guo, YD Luo, J Xu; (III) Provision of study materials or patients: YL Shu, H Yu; (IV) Collection and assembly of data: YL Shu, H Yu, YP Huang, WL Jiang; (V) Data analysis and interpretation: YL Shu, H Yu, YD Luo, J Xu; (VI) Manuscript writing: All authors; (VII) Final approval of manuscript: All authors.

[#]These authors contributed equally to this work.

[*]These authors contributed equally to this work.

Correspondence to: Jie Xu, MD; Yin-Deng Luo, MD. Department of Radiology, The Second Affiliated Hospital of Chongqing Medical University, 74 Chongqing Linjiang Road, Chongqing 400010, China. Email: xj304847@cqmu.edu.cn; 300757@hospital.cqmu.edu.cn.

Background: Currently, the traditional chest computed tomography (CT) scan mode presents certain limitations in evaluating the coronary artery calcification score (CACS). Therefore, this study aimed to investigate the impact of using the Turbo FLASH mode to optimize chest CT on radiation dose, image quality, and CACS.

Methods: In this cross-sectional study, a total of 968 patients who simultaneously underwent routine chest CT (using the Turbo FLASH mode or the conventional mode) and cardiac CT [coronary calcium scan (CCS) and coronary CT angiography] were retrospectively collected. A comparative analysis was performed between the FLASH mode (n=493) and the conventional mode (n=475) in terms of radiation dose and image quality. CACS analysis was carried out using a semi-automatic software based on CCS, chest CT (FLASH), and chest CT (conventional). Using the CCS-CACS as a reference, the correlation, consistency, and concordance rate of risk categories based on CACS from the two chest CT modes were independently calculated.

Results: Chest CT (FLASH) reduced the mean radiation dose by 36.47 mGy·cm (11.1%) and exhibited fewer motion artifacts, albeit with a worse signal-to-noise ratio (SNR) (all P<0.05). For CACS quantification, chest CT (FLASH) showed a stronger linear correlation (r, 0.998 *vs.* 0.941) and higher consistency (mean difference, −5.653 *vs.* 7.142) compared to chest CT (conventional). For risk categories, chest CT (FLASH) set also demonstrated a higher concordance rate [91.3% (450/493) *vs.* 84% (399/475)]. Specifically, category 1 (CACS 1–10) exhibited the most significant improvement (78.5% *vs.* 53.5%). Additionally, chest CT (FLASH) had a lower false-negative rate [1% (5/493) *vs.* 4.6% (22/475)].

Conclusions: The Turbo FLASH mode of chest CT excels in detecting microcalcifications, reducing false negatives, and improving the accuracy of risk categories. It also lowers radiation exposure, but it may compromise the SNR of images.

^ ORCID: Ying-Lan Shu, 0009-0007-1572-0800; Han Yu, 0009-0007-9627-5939; Da-Jing Guo, 0000-0001-8655-6621; Ya-Ping Huang, 0009-0007-3079-9967; Wen-Li Jiang, 0009-0002-5102-5972; Yin-Deng Luo, 0000-0001-8720-8418; Jie Xu, 0000-0002-2523-7915.

Keywords: Coronary artery disease (CAD); vascular calcification; coronary calcium scan (CCS); cardiovascular risk score; radiation dose

Submitted May 23, 2024. Accepted for publication Jan 21, 2025. Published online Feb 26, 2025.
doi: 10.21037/qims-24-1005
View this article at: https://dx.doi.org/10.21037/qims-24-1005

Introduction

Coronary artery disease (CAD) is the primary cause of premature mortality, significantly burdening the global healthcare system (1,2). Coronary artery calcium (CAC), as a marker and an early indicator of CAD (3), is typically quantified via the coronary artery calcification score (CACS) (4). Clinically, CACS is obtained through a non-enhanced coronary calcium scan (CCS) (5-7), which is often conducted alongside coronary computed tomography (CT) angiography to provide a comprehensive assessment of cardiovascular stenosis and calcification, rather than as a standalone procedure. The complexity and high cost of these exams, coupled with the prolonged asymptomatic phase of CAD (7), frequently result in delayed CAC measurements for patients.

Utilizing routine non-gated chest CT scans for CACS quantification offers a potential solution to these challenges, avoiding additional radiation exposure and economic burden, especially in the context of widespread low-dose CT lung cancer screening programs. However, the accuracy of CACS assessment using chest CT is still debated, with previous meta-analyses reporting significant false-negative rates (8.8%) (8), mainly due to the inability to suppress coronary motion artifacts. However, with advances in CT technology, improving the temporal resolution of chest CT may be a potentially feasible solution (9-13).

The ultra-fast Turbo FLASH mode of dual-source CT (DSCT), which employs two X-ray tubes and detectors, stands out as the optimal choice for temporal resolution and has demonstrated highly consistent CACS results between chest CT (FLASH) and CCS (12,13). However, previous studies (12,13) have primarily compared the performance of CACS between chest CT (FLASH) and CCS, rarely including a conventional chest CT group for comparison. Although the faster scan mode helps reduce motion artifacts and radiation exposure (14), it may also compromise image resolution and increase quantum noise (15,16). Therefore, a comprehensive assessment of the advantages and disadvantages of this technology is essential.

In this study, we aimed to address these knowledge gaps by analyzing data from chest CT (FLASH) and chest CT (conventional) acquired on DSCT systems. Our primary objectives were to compare the radiation dose and image quality between the two modes, as well as evaluate their performance in CACS quantification and risk stratification. By highlighting the incremental value of the Turbo FLASH mode in chest CT for CAD screening, our findings contribute to improving the accuracy of CACS assessment in a dual-risk screening setting. We present this article in accordance with the STROBE reporting checklist (available at https://qims.amegroups.com/article/view/10.21037/qims-24-1005/rc).

Methods

Study sample

This retrospective study was approved by the Ethics Committee of the Second Affiliated Hospital of Chongqing Medical University (No. 2022-10) and was conducted in accordance with the Declaration of Helsinki (as revised in 2013). The requirement for written informed consent was waived by the Ethics Committee due to the nature of the retrospective design.

We recruited patients who underwent clinically indicated routine chest CT and cardiac CT examinations (CCS and coronary CT angiography) during the same examination period at the Second Affiliated Hospital of Chongqing Medical University between January 2022 and March 2023. These chest CT scans were performed to evaluate chest-related diseases, for health screenings, and for other clinical reasons. Cardiac CTs were conducted in patients with a history of chest pain to assess potential CAD, as well as for follow-up in those with known CAD. Patients were excluded from the study based on the following criteria: (I) a history of percutaneous coronary intervention (PCI), coronary artery bypass grafting (CABG), or metal implantation; (II) chest CT exams that included adjacent body parts, making it impossible to independently calculate the radiation dose for the chest CT. A radiologist accessed patient information using the Hospital Information System

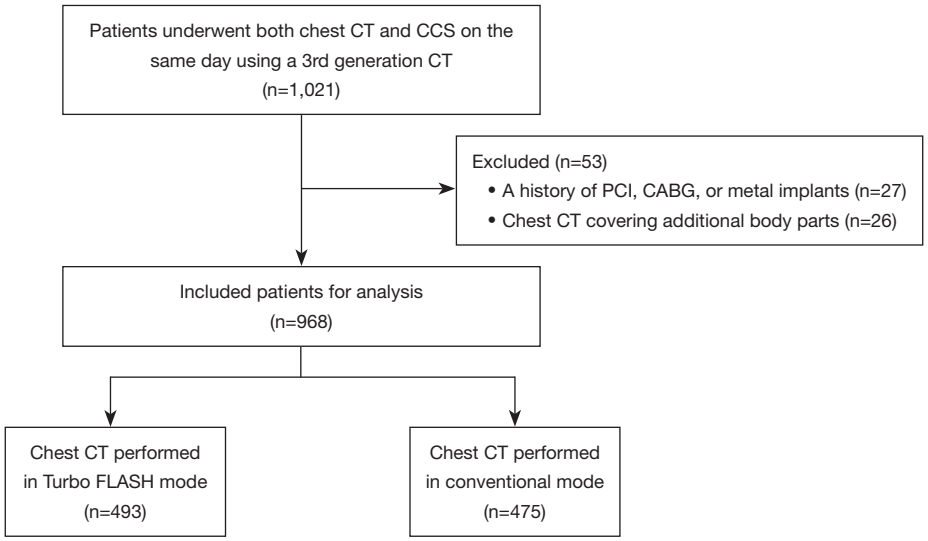

Figure 1 Flowchart of the included patients. CT, computed tomography; CCS, coronary calcium scan; PCI, percutaneous coronary intervention; CABG, coronary artery bypass grafting.

(*Figure 1*). Ultimately, a total of 968 patients were reviewed, comprising 493 in the chest CT (FLASH) group and 475 in the chest CT (conventional) group based on the different CT modalities.

CT acquisition

All imaging data were acquired from two DSCT systems (Somatom Force and Somatom Drive; Siemens Healthcare, Erlangen, Germany). The chest CT scans covered the entire lung volume, extending from the upper thoracic apex to the inferior margin of the diaphragm. The CCS comprehensively encompassed the heart, extending from 1 cm below the tracheal bifurcation to the diaphragmatic surface. Scanning parameters for chest CT (FLASH), chest CT (conventional), and CCS performed on these two CT systems are detailed in *Table 1*. The dose-length product (DLP) values for both chest CT and CCS were obtained from individual dose reports within the picture archiving and communication system (PACS).

CT image reconstruction and analysis

For all image analyses, the reconstructed series of chest CT [with harmonized parameters, including a slice thickness of 1 mm and an increment of 0.7 mm for chest (FLASH) and both a slice thickness and increment of 1 mm for chest (conventional)] and CCS (with a slice thickness of 3 mm and an increment of 1.5 mm) were transferred to a Siemens syngo MMWP VE36A workstation. Image quality was assessed through a combined subjective and objective evaluation. Two radiologists, each with over five years of experience in cardiac imaging, conducted all image analyses and measurements collaboratively. In cases of discrepancies or differing opinions, the radiologists held additional consultations to reach a consensus.

Chest CT images analysis

Based the 1975 American Heart Association coronary classification, the coronary arteries in chest CT images were segmented into 18 sections for subjective evaluation (17,18). A scoring system was employed to rate coronary artery segments with diameters exceeding 1.5 mm, according to the following criteria: 1 (excellent): no artifacts, with ≥14 segments; 2 (good): 9–13 segments; 3 (moderate): 4–8 segments; 4 (bad): <4 segments.

The evaluation of general chest CT images incorporated both subjective and objective assessments (*Figure 2*). Subjectively, the fine structure was assessed using a 3-point scale based on lung window settings (window width 1,200; window center −600), as follows:

- Score of "1": slightly blurred structure with artifacts in the lung texture and field, but still diagnostic;
- Score of "2": fine structure with good contrast, slight artifacts, and some blurring of lung texture;

Table 1 Scan parameters of chest CT (FLASH), chest CT (conventional), and CCS

Index	Chest CT (FLASH)		Chest CT (conventional)		CCS	
	Drive	Force	Drive	Force	Drive	Force
Tube voltage (kV)	120	120	120	120	120	120
Tube current (mAs)	CARE Dose4 (Ref. 250)	CARE Dose4 (Ref. 150)	CARE Dose4 (Ref. 150)	CARE Dose4 (Ref. 80)	CARE Dose4 (Ref. 80)	CARE Dose4 (Ref. 80)
Rotation time (s/rot)	0.28	0.25	0.5	0.5	0.28	0.25
Pitch	2.7	2.7	1.2	1.2	*	*
Scan field of view (cm)	33.2	38.6	50	50	*	*
Collimation (mm)	2×128×0.6	2×192×0.6	128×0.6	192×0.6	128×0.6	192×0.6
Slice thickness (mm)	1	1	1	1	3	3
Slice increment (mm)	0.7	0.7	1	1	1.5	1.5
Iterative reconstruction	ADMIRE3	ADMIRE4	ADMIRE3	ADMIRE4	FBP	FBP
Convolution algorithm	Br37	Bf40	Bf38	Bf40	Qr36	Qr36
Scanned phase of the cardiac cycle (R-R interval)	–	–	–	–	70% (HR <75 bmp), 40% (HR ≥75 bpm)	70% (HR <75 bmp), 40% (HR ≥75 bpm)

*, changes as heart rate fluctuates. CT, computed tomography; CCS, coronary calcium scan; CARE Dose4, automatic tube current modulation; Ref., reference; ADMIRE, advanced modeled iterative reconstruction algorithm; FBP, filtered back projection; HR, heart rate.

- Score of "3": clear display of fine structure with excellent contrast, sharp edges, and detailed lung texture.

For the objective evaluation, mediastinum window settings (window width 400; window center 40) were utilized to measure signal-to-noise ratio (SNR) and contrast-to-noise ratio (CNR). At the four-chambered cardiac slice of the chest CT, three regions of interest (ROIs, 100 mm^2) were positioned within the mediastinum, and another three ROIs (20–30 mm^2) were placed within subcutaneous fat. The mean CT number (Hounsfield units, HU) from the three mediastinal ROIs was denoted as $HU_{soft\ tissue}$, and its standard deviation (SD) was labeled as $SD_{soft\ tissue}$. The mean CT number from the three fat ROIs was defined as HU_{fat}, and its SD was referred to as $SD_{background}$. SNR and CNR were then calculated using the following formulas:

$$SNR = HU_{soft\ tissue} / SD_{soft\ tissue} \quad [1]$$

$$CNR = \left(HU_{soft\ tissue} - HU_{fat}\right) / SD_{background} \quad [2]$$

CACS quantitation and risk category analysis

The calcified areas (CT number ≥130 HU, area ≥1 mm^2) within each coronary artery segment were identified and labeled using the workstation, contributing to the overall CACS (4). Based on the total CACS, five risk categories were established: category 0 (CACS 0, no or very low risk), category 1 (CACS 1–10, low risk), category 2 (CACS 11–100, mild risk), category 3 (CACS 101–400, moderate risk), and category 4 (CACS >400, severe risk) (19).

Statistical analysis

The statistical analyses were performed using the software SPSS 26.0 (IBM Corp., Armonk, NY, USA) and MedCalc Version 20.2 (MedCalc, Ostend, Belgium). Continuous data were analyzed for normal distribution using the Shapiro-Wilk test. Data that followed a normal distribution were presented as mean and standard deviation (mean ± SD) and compared between groups using the independent samples *t*-test. Skewed data were expressed as medians with interquartile ranges (IQRs), and group comparisons were made using the Mann-Whitney *U* test. Categorical variables were reported as frequencies and analyzed among groups using the chi-square test or Fisher's exact test. A significance level of $P<0.05$ was considered statistically significant. The correlation of CACS between CCS and chest CT (FLASH)

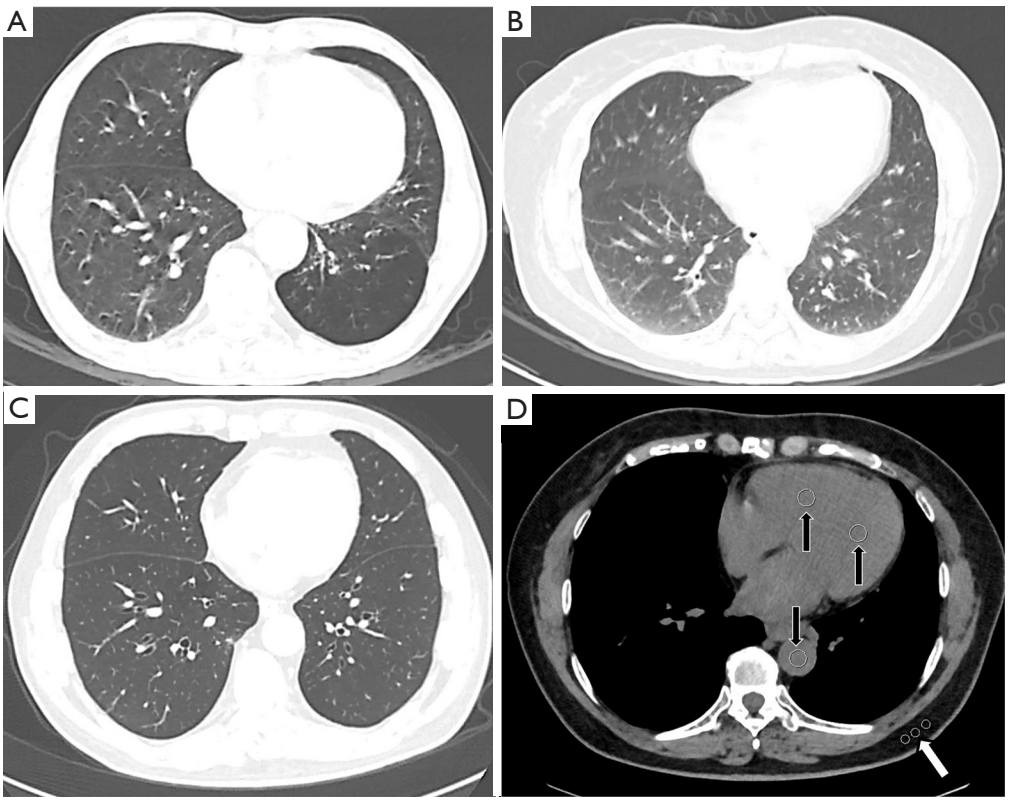

Figure 2 Representative images with subjective and objective evaluations. (A) The representative image of 1 point in the subjective fine structure evaluation: the structure was slightly blurred with artifacts in the lung texture and lung field, but the image could be used for diagnosis. (B) The representative image with 2 points: with good contrast, slight artifacts, and blurring of lung texture. (C) The representative image with 3 points: clear display of fine structure with excellent contrast, sharp and clear edges of lung texture. (D) The representative image with the objective evaluation. The mediastinum (black arrows) and subcutaneous fat (white arrow) were measured separately.

or chest CT (conventional) was determined using the Spearman correlation coefficient. Bland-Altman plots were used to present bias and limits of agreement within the 95% confidence interval. Kappa analysis was performed to assess agreement in risk categorization between two sets of data.

Results

Demographics and clinical characteristics

No significant difference was observed in clinical characteristics and traditional CAD risk factors between chest CT (FLASH) set and chest CT (conventional) set (*Table 2*).

Radiation dose and image quality assessment

The median radiation dose for CCS was 114.1 (IQR, 84.75–158.3) mGy·cm. In comparison, chest CT scans had more than double this dose: 281.4 (IQR, 248.85–319.5) mGy·cm for FLASH mode and 304.6 (IQR, 246.45–381.6) mGy·cm for conventional mode. Among the enrolled patients, 74.2% (366/493) demonstrated good coronary artery quality (scoring 1 or 2) in the chest CT (FLASH) set, whereas this value was only 15.4% (73/475) in the chest CT (conventional) set. To visually compare coronary images between chest CT (FLASH), chest CT (conventional), and CCS (*Figure 3*), we searched among 968 participants and found 17 who underwent three CT exams within three months. The FLASH mode did manage to prevent motion artifact caused by failure breath-holding while achieving superior fine structure scores in the chest CT (FLASH) set ($P<0.05$). The CNR was not statically significant between chest CT (FLASH) set and chest CT

Table 2 Clinical characteristics of the FLASH and the conventional sets

Clinical characteristics	FLASH (n=493)	Conventional (n=475)	χ^2/Z value	P value
Gender			0.001†	0.977
Male	262 (53.1)	252 (53.1)		
Female	231 (46.9)	223 (46.9)		
Age (years)	60 [54–69]	60 [53–69]	–0.071‡	0.943
Heart rate (beats per minute)	68 [57–79]	69 [60–80]	–1.541‡	0.123
Body mass index (kg/m^2)	21.1 [19.1–23.2]	20.7 [18.71–23.01]	–1.38‡	0.168
Smoking	183 (37.12)	188 (39.58)	0.618†	0.432
Drinking	191 (38.74)	179 (37.68)	0.115†	0.735
Hypertension	236 (47.87)	249 (52.42)	1.793†	0.181
Diabetes	154 (31.24)	175 (36.84)	3.384†	0.066
Hyperlipidemia	260 (52.74)	238 (50.11)	0.671†	0.413

Data are presented as n (%) or median [IQR]. †, Chi-squared test; ‡, Mann-Whitney *U* test; IQR, interquartile range.

(conventional) set (P=0.708). Nevertheless, SNR in chest CT (FLASH) was slightly inferior than that in chest CT (conventional) (median SNR 21.02 *vs.* 25.54; P<0.05) (*Table 3*).

Quantification of CACS

The false negatives in chest CT (conventional) set outnumbered those in chest CT (FLASH) set at 22 cases versus five cases. Spearman's rank correlation coefficient was used to determine the correlation of CACS between chest CT and CCS, yielding r=0.998 (P<0.05) for the chest CT (FLASH) set and r=0.941 (P<0.05) for the chest CT (conventional) set (*Figure 4*). The Bland-Altman plot (CACS of chest CT minus CCA-CACS) revealed a mean difference of –5.653 and 95% limits of agreement of –52.144 to 40.839 in the chest CT (FLASH) set, whereas the results had a mean difference of 7.142 and 95% limits of agreement of –247.678 to 261.962 in the chest CT (conventional) set (*Figure 4*).

Risk categorization

The risk categorization between CCS-CACS and the CACS of chest CT (the FLASH set and the conventional set) is shown in the confusion matrices in *Table 4*. Analysis of the weighted kappa results revealed a higher level of consistency in risk category for the chest CT (FLASH) set (κ=0.929) compared to the chest CT (conventional) set (κ=0.874). In terms of misclassification, there were 43 (8.7%) reported cases in the chest CT (FLASH) set and 76 cases (16%) in the chest CT (conventional) set.

Discussion

To enable chest CT for dual-risk screening (lung cancer and CAD), the optimization of scanning protocol should be considered comprehensively. This encompasses factors such as radiation dose, image quality for both lung and coronary, and performance on CACS.

Radiation dose reduction and image quality impact

In CT scans, radiation dose is influenced by various factors, including protocols, scanning parameters, scan duration, and patient sample size (20-22). Consequently, studies have shown a wide range of DLP values, from the low tens to over 600 mGy·cm for chest CT (12,13,23-27), and DLP typically remains below 50 mGy·cm for cardiac CT (13,28,29). Our results indicated relatively high radiation dose levels for both the heart with 114.1 (IQR, 84.75–158.3) mGy·cm and chest with 281.4 (IQR, 248.85–319.5) mGy·cm. We reasonably speculate that this elevation was caused by high tube current settings of 80 mAs or more in our CT protocols, compared to the typical range of 20–60 mAs used in low-dose protocols (12,13). The high reference mAs setting might enhance image quality, especially for patients with cardiovascular and pulmonary

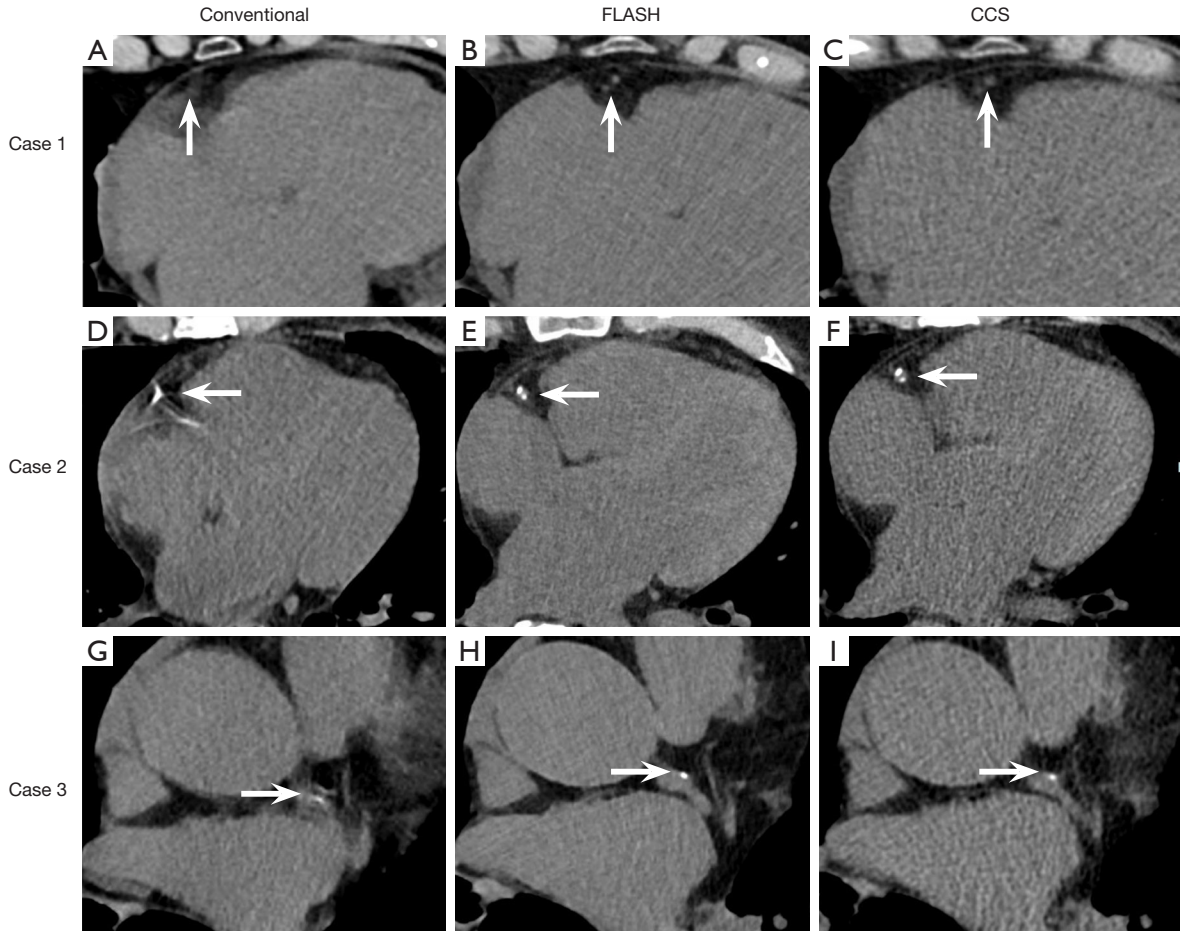

Figure 3 Representative images of coronary image quality from three scanning methods. To visually compare coronary image quality among three CT examinations, namely, chest CT (FLASH), chest CT (conventional), and CCS, we identified eligible patients who underwent all three scans within three months using the hospital information system. A limited number of patients met the criteria, and three cases with representative coronary artery segments (arrows) are presented in the figure above. (A-C) Case 1: no calcified plaques present. (D-F) Case 2: presence of calcium plaques. (G-I) Case 3: a calcified plaque was detected on chest CT (FLASH) (H) and CCS (I) but was missed by chest CT (conventional) (G). CT, computed tomography; CCS, coronary calcium scan.

histories. Additionally, for chest CT, over scanning was noted in patients who had difficulty holding their breath, and some were unable to raise their arms, resulting in increased automatic tube current exposure (30).

FLASH mode is Siemens' unique dual-tube, dual-detector ultra-fast CT scanning technology. Our study demonstrated an 11.1% (36.47 mGy·cm) reduction in radiation dose with chest CT using FLASH mode. However, doses remained high due to the reference mAs settings. This can be addressed through the optimization of scanning parameters. In a low-dose protocol utilizing an ultra-low reference mAs of 20 for FLASH mode, it achieved a DLP of only 58.7±18.4 mGy·cm for chest CT (13).

Further reduction in radiation dose can be achieved through various reconstruction techniques. The system can be optimized by integrating advanced methods, such as deep learning algorithms and precise scanning positioning technologies. Deep learning image reconstruction (DLIR) has been reported to reduce doses by 50% or more while maintaining image quality (24,31-33). Additionally, three-dimensional (3D) landmark scanning technology can minimize over scanning by accurately targeting organs, potentially decreasing scan length by 12.7 mm and reducing radiation dose by 11.9% for chest CT scans (23).

Moreover, the ultra-high temporal resolution of the Turbo FLASH mode effectively mitigates motion artifacts in

Table 3 The radiation dose and image quality of chest CT (FLASH) and chest CT (conventional)

Parameters	FLASH (n=493)	Conventional (n=475)	χ^2/Z/t value	P value
DLP (mGy·cm)	281.4 [248.85–319.5]	304.6 [246.45–381.6]	−4.556†	<0.001
Coronary artery quality				
1	186 (37.7)	5 (1.1)	205.242‡	<0.001
2	180 (36.5)	68 (14.3)	62.475‡	<0.001
3	102 (20.7)	170 (35.8)	26.577‡	<0.001
4	25 (5.1)	232 (48.8)	237.432‡	<0.001
Fine structure	2.98±0.15	2.91±0.29	−4.594§	<0.001
SNR	21.02 [12.17–29.87]	25.54 [12.92–38.17]	−2.708†	0.007
CNR	52.38 [29.15–75.6]	55.55 [27.6–83.49]	−0.374†	0.708

Data are presented as median [IQR], n (%) or mean ± SD. Fine structure using 3-point Likert scale (1, the structure was slightly blurred with artifacts in the lung texture and lung field, but the image could be used for diagnosis; 2, fine structure with good contrast, slight artifacts, and blur of lung texture; 3, clear display of fine structure with excellent contrast, sharp and clear edges of lung texture). †, Mann-Whitney *U* test; ‡, Chi-squared test; §, independent samples *t*-test. CT, computed tomography; DLP, dose-length product; SNR, signal-to-noise ratio; CNR, contrast-to-noise ratio; IQR, interquartile range; SD, standard deviation.

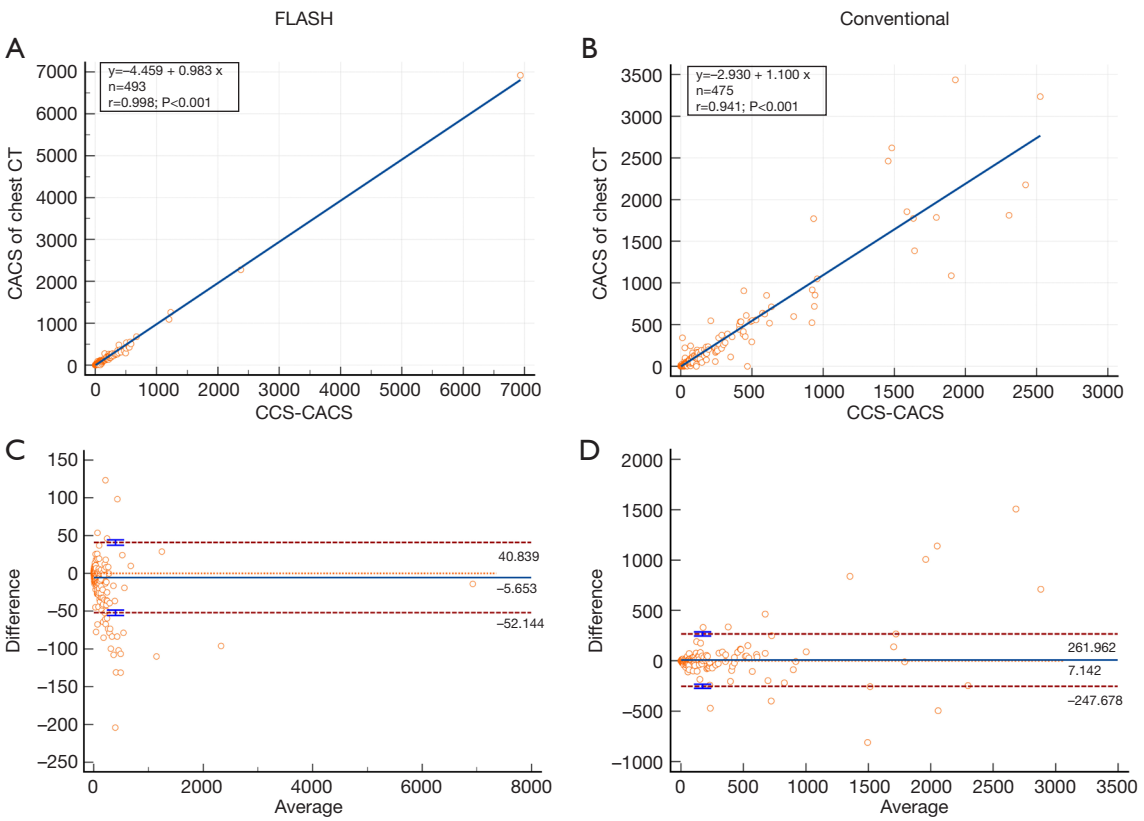

Figure 4 Scatter plots and Bland-Altman plots for chest CT (FLASH) and chest CT (conventional). Scatter plots illustrate the correlation of CACS in chest CT (FLASH) (A) and chest CT (conventional) (B). Bland-Altman plots display the bias and 95% limits of agreement for CACS in chest CT (FLASH) (C) and chest CT (conventional) (D). CT, computed tomography; CACS, coronary artery calcification score.

Table 4 Confusion matrices of risk categories between the chest CT and CCS

Chest CT categories	CCS categories (ref.)					Total	Underestimation	Overestimation	Concordance
	0	1	2	3	4				
FLASH									
0	264	5	0	0	0	269	5 (1.9)	–	264 (98.1)
1	5	51	9	0	0	65	9 (13.8)	5 (7.7)	51 (78.5)
2	0	7	76	9	0	92	9 (9.8)	7 (7.6)	76 (82.6)
3	0	0	2	48	5	55	5 (9.1)	2 (3.6)	48 (87.3)
4	0	0	0	1	11	12	–	1 (8.3)	11 (91.7)
Total	269	63	87	58	16	493	28 (5.7)	15 (3.0)	450 (91.3)
Conventional									
0	270	19	3	0	0	292	22 (7.5)	–	270 (92.5)
1	4	23	16	0	0	43	16 (37.2)	4 (9.3)	23 (53.5)
2	0	8	45	9	0	62	9 (14.5)	8 (12.9)	45 (72.6)
3	0	0	10	29	5	44	5 (11.4)	10 (22.7)	29 (65.9)
4	0	0	0	2	32	34	–	2 (5.9)	32 (94.1)
Total	274	50	74	40	37	475	52 (10.9)	24 (5.1)	399 (84.0)

Values are n or n (%). Category 0, CACS 0; Category 1, CACS 1–10; Category 2, CACS 11–100; Category 3, CACS 101–400; Category 4: CACS >400. CT, computed tomography; CCS, coronary calcium scan; Ref., reference; CACS, coronary artery calcification score.

both lung parenchyma and coronary arteries, a longstanding limitation of non-gated chest CT for CAD screening (8). Although the Turbo FLASH mode excels in motion artifact suppression, it is crucial to assess its potential impact on image quality. Consistent with a previous report (34), our objective evaluation revealed a slight decrease in SNR in the chest CT (FLASH) dataset. However, it is noteworthy that no significant deterioration was observed in the CNR. This discrepancy can be attributed to the differing tissue types used for noise calculation, where soft tissue is employed for SNR and subcutaneous fat for CNR. The lower attenuation of subcutaneous fat renders it less prone to artifacts or increased noise induced by high pitch values (35).

CACS quantification

The accurate quantification of CACS and the subsequent risk stratification based on CACS thresholds are pivotal components in the comprehensive evaluation and management of cardiovascular disease risk. In this part, we focused on assessing the performance of the Turbo FLASH mode in chest CT for CACS quantification and risk categorization, in comparison to the conventional chest CT mode.

Unlike the interval scanning (36,37), our participants had undergone chest CT and CCS scans in the same examination, thus eliminating the potential impact of CACS changes over time. Regarding CACS quantification, the chest CT (FLASH) set demonstrated superior performance compared to the chest CT (conventional) in terms of linear correlation (r, 0.998 *vs.* 0.941) and consistency [mean difference −5.653 *vs.* 7.142; 95% limits of agreement (−52.144 to 40.839) *vs.* (−247.678 to 261.962)]. This robust correlation and high consistency underscore the reliability and accuracy of the Turbo FLASH mode in quantifying coronary artery calcifications.

Risk categorization

The primary aim of accurately quantifying CACS in chest CT is to facilitate risk categorization CAD. In our study, we classified the degree of calcification into five categories based on the total CACS. Overall, the Turbo FLASH mode displayed a superior concordance rate in risk categorization using CACS thresholds compared to the conventional mode (91.3% *vs.* 84%).

Across each specific category, the Turbo FLASH mode

demonstrated remarkable consistency in risk classification. For category 0 (CACS 0), representing the absence of coronary calcification, the concordance rate was 98.1% (264/269) for the Turbo FLASH set and 92.5% (270/292) for the conventional set. This consistency in category 0 is paramount in evaluating the performance of CAC screening exams, as CACS 0 serves as a crucial cut-off point for initiating primary prevention measures (38). Furthermore, the Turbo FLASH mode showed the most significant improvement in the concordance rate for category 1 (CACS 1–10), which comprises microcalcifications that are often challenging to diagnose accurately in clinical settings. Specifically, the Turbo FLASH set achieved a concordance rate of 78.5% (51/65), whereas the conventional set only achieved 53.5% (23/43). Additionally, the Turbo FLASH mode maintained its superiority in the concordance rate for categories 2 (CACS 11–100) and 3 (CACS 101–400), achieving 82.6% (76/92) and 87.3% (48/55) respectively, compared to 72.6% (45/62) and 65.9% (29/44) for the conventional set. However, in category 4 (CACS >400), representing severe coronary calcification, the concordance rates between the two CT sets were similar, with a slight decrease in the Turbo FLASH set [91.7% (11/12) *vs.* 94.1% (32/34)]. Nevertheless, this similarity could be attributed to the small sample size in category 4, with only a few misclassified cases in each group.

In summary, our study demonstrated that the Turbo FLASH mode outperforms the conventional chest CT in the consistency of risk classifications from category 0 to 3, covering the range from no calcification to moderate CACS. This improved consistency in risk categorization is crucial for guiding clinical decision-making and implementing appropriate preventive measures in individuals with varying degrees of coronary artery calcification (6,39).

Analysis of risk categorization error cases

The chest CT (FLASH) set exhibited a significantly lower number of misclassification cases (43/493, 8.7% *vs.* 76/475, 16%) compared to the chest CT (conventional) set. These cases were wrongly assigned into adjacent risk categories in the chest CT (FLASH) set, whereas in the chest CT (conventional) set, three cases (3/475, 0.6%) were misclassified across groups, specifically from category 2 [11–100] to category 0 (CACS 0). The accuracy of risk category assignments is crucial as it directly impacts the intensity of risk management strategies (38), and thus, misclassification across groups may have more severe adverse effects on patients.

Furthermore, our results indicate that the majority of misclassified cases were underestimated, regardless of whether the FLASH mode (28/43, 65.1%) or the conventional mode (52/76, 68.4%) was used. Among these, five false negatives (1%) were observed in the chest CT (FLASH) set, and 22 false negatives (4.6%) in the chest CT (conventional) set. Notably, these false negatives had fairly low CACS values (2.46±4.08) and were accompanied by significant motion artifacts surrounding calcified plaques. These artifacts led to blurring of microcalcifications, ultimately resulting in reduced density and failure to recognize calcification, as exemplified in case 3 of *Figure 3*. Consequently, the chest CT (FLASH) modality can effectively reduce the false-negative rate (from 4.6% to 1%) by suppressing coronary motion artifacts.

The remaining misclassified cases were overrated, comprising 15 in the chest CT (FLASH) set and 24 in the chest CT (conventional) set. Of these, 83.3% (20/24) were non-zero CACS cases with relatively high CACS values (68.63±81.58) and severe motion artifacts. These artifacts contributed to an increase in the apparent volume of macrocalcification, as illustrated in *Figure 3*, case 2. In sum, motion artifact is the primary cause of misclassification, and the CT (FLASH) modality can significantly enhance the detection of microcalcifications and mitigate the occurrence of false negatives.

This study has several limitations that must be acknowledged. Firstly, since the two chest CT modes were performed separately, the results may be influenced by potential individual differences among the participants. However, we conducted a comparative analysis of the clinical characteristics between the two chest CT sets and found no statistically significant differences. Secondly, the limited number of cases with CACS >400 in this study necessitates the expansion of the sample size in future follow-up research to enhance the accuracy of the experimental results. Thirdly, the retrospective nature of the study limited our ability to compare radiation dose and image quality across different pitches, advanced post-processing reconstruction techniques, and precise scanning positioning technologies. This aspect will be further explored and incorporated in subsequent studies.

Conclusions

The utilization of Turbo FLASH mode in DSCT for the assessment of CACS in chest CT images emerges as a promising technical strategy, offering three distinct

advantages. Firstly, it effectively reduces radiation dose and mitigates motion artifacts. Secondly, it significantly decreases the false-negative rate for coronary calcium screening. Lastly, chest CT using Turbo FLASH mode demonstrates superior performance in risk stratification especially for individuals with microcalcifications. Notably, excessive pitch can reduce SNR of the chest CT images. Therefore, it is crucial to strike a balance between image quality and clinical requirements when setting scan parameters.

Acknowledgments

This work was supported by all the reviewers who participated in the review and MJEditor (www.mjeditor.com) for its linguistic assistance during the preparation of this manuscript.

Footnote

Reporting Checklist: The authors have completed the STROBE reporting checklist. Available at https://qims.amegroups.com/article/view/10.21037/qims-24-1005/rc

Funding: This work was supported by the Kuanren Talents Program of the Second Affiliated Hospital of Chongqing Medical University (Nos. 2020-7 and 2021-24) and the General Project of Technological Innovation and Application Development Project of Chongqing Science and Technology Bureau (No. cstc2019jscx-msxmX0253).

Conflicts of Interest: All authors have completed the ICMJE uniform disclosure form (available at https://qims.amegroups.com/article/view/10.21037/qims-24-1005/coif). The authors have no conflicts of interest to declare.

Ethical Statement: The authors are accountable for all aspects of the work in ensuring that questions related to the accuracy or integrity of any part of the work are appropriately investigated and resolved. This retrospective study was approved by the Ethics Committee of the Second Affiliated Hospital of Chongqing Medical University (No. 2022-10) and was conducted in accordance with the Declaration of Helsinki (as revised in 2013). The requirement for written informed consent was waived by the ethics committee due to the nature of the retrospective design.

References

1. Tsao CW, Aday AW, Almarzooq ZI, Anderson CAM, Arora P, Avery CL, et al. Heart Disease and Stroke Statistics-2023 Update: A Report From the American Heart Association. Circulation 2023;147:e93-e621. Erratum in: Circulation 2023;147:e622. Erratum in: Circulation 2023;148:e4.
2. Shahjehan RD, Sharma S, Bhutta BS. Coronary Artery Disease. 2024 Oct 9. In: StatPearls [Internet]. Treasure Island (FL): StatPearls Publishing; 2025.
3. Golub IS, Termeie OG, Kristo S, Schroeder LP, Lakshmanan S, Shafter AM, Hussein L, Verghese D, Aldana-Bitar J, Manubolu VS, Budoff MJ. Major Global Coronary Artery Calcium Guidelines. JACC Cardiovasc Imaging 2023;16:98-117.
4. Agatston AS, Janowitz WR, Hildner FJ, Zusmer NR, Viamonte M Jr, Detrano R. Quantification of coronary artery calcium using ultrafast computed tomography. J Am Coll Cardiol 1990;15:827-32.
5. Greenland P, Bonow RO, Brundage BH, Budoff MJ, Eisenberg MJ, Grundy SM, Lauer MS, Post WS, Raggi P, Redberg RF, Rodgers GP, Shaw LJ, Taylor AJ, Weintraub WS; American College of Cardiology Foundation Clinical Expert Consensus Task Force (ACCF/AHA Writing Committee to Update the 2000 Expert Consensus Document on Electron Beam Computed Tomography); Society of Atherosclerosis Imaging and Prevention; Society of Cardiovascular Computed Tomography. ACCF/AHA 2007 clinical expert consensus document on coronary artery calcium scoring by computed tomography in global cardiovascular risk assessment and in evaluation of patients with chest pain: a report of the American College of Cardiology Foundation Clinical Expert Consensus Task Force (ACCF/AHA Writing Committee to Update the 2000 Expert Consensus Document on Electron Beam Computed Tomography) developed in collaboration with

the Society of Atherosclerosis Imaging and Prevention and the Society of Cardiovascular Computed Tomography. J Am Coll Cardiol 2007;49:378-402.
6. Hecht HS, Cronin P, Blaha MJ, Budoff MJ, Kazerooni EA, Narula J, Yankelevitz D, Abbara S. 2016 SCCT/STR guidelines for coronary artery calcium scoring of noncontrast noncardiac chest CT scans: A report of the Society of Cardiovascular Computed Tomography and Society of Thoracic Radiology. J Cardiovasc Comput Tomogr 2017;11:74-84.
7. Greenland P, Alpert JS, Beller GA, Benjamin EJ, Budoff MJ, Fayad ZA, et al. 2010 ACCF/AHA guideline for assessment of cardiovascular risk in asymptomatic adults: a report of the American College of Cardiology Foundation/American Heart Association Task Force on Practice Guidelines. J Am Coll Cardiol 2010;56:e50-103.
8. Xie X, Zhao Y, de Bock GH, de Jong PA, Mali WP, Oudkerk M, Vliegenthart R. Validation and prognosis of coronary artery calcium scoring in nontriggered thoracic computed tomography: systematic review and meta-analysis. Circ Cardiovasc Imaging 2013;6:514-21.
9. Shin JM, Kim TH, Kim JY, Park CH. Coronary artery calcium scoring on non-gated, non-contrast chest computed tomography (CT) using wide-detector, high-pitch and fast gantry rotation: comparison with dedicated calcium scoring CT. J Thorac Dis 2020;12:5783-93.
10. Wu MT, Yang P, Huang YL, Chen JS, Chuo CC, Yeh C, Chang RS. Coronary arterial calcification on low-dose ungated MDCT for lung cancer screening: concordance study with dedicated cardiac CT. AJR Am J Roentgenol 2008;190:923-8.
11. Chen Y, Hu Z, Li M, Jia Y, He T, Liu Z, Wei D, Yu Y. Comparison of Nongated Chest CT and Dedicated Calcium Scoring CT for Coronary Calcium Quantification Using a 256-Dector Row CT Scanner. Acad Radiol 2019;26:e267-74.
12. Hutt A, Duhamel A, Deken V, Faivre JB, Molinari F, Remy J, Remy-Jardin M. Coronary calcium screening with dual-source CT: reliability of ungated, high-pitch chest CT in comparison with dedicated calcium-scoring CT. Eur Radiol 2016;26:1521-8.
13. Xia C, Vonder M, Pelgrim GJ, Rook M, Xie X, Alsurayhi A, van Ooijen PMA, van Bolhuis JN, Oudkerk M, Dorrius M, van der Harst P, Vliegenthart R. High-pitch dual-source CT for coronary artery calcium scoring: A head-to-head comparison of non-triggered chest versus triggered cardiac acquisition. J Cardiovasc Comput Tomogr 2021;15:65-72.
14. Agostini A, Borgheresi A, Carotti M, Ottaviani L, Badaloni M, Floridi C, Giovagnoni A. Third-generation iterative reconstruction on a dual-source, high-pitch, low-dose chest CT protocol with tin filter for spectral shaping at 100 kV: a study on a small series of COVID-19 patients. Radiol Med 2021;126:388-98.
15. Balata H, Blandin Knight S, Barber P, Colligan D, Crosbie EJ, Duerden R, et al. Targeted lung cancer screening selects individuals at high risk of cardiovascular disease. Lung Cancer 2018;124:148-53.
16. Li D, Ma L, Li J, Qi S, Yao Y, Teng Y. A comprehensive survey on deep learning techniques in CT image quality improvement. Med Biol Eng Comput 2022;60:2757-70.
17. Austen WG, Edwards JE, Frye RL, Gensini GG, Gott VL, Griffith LS, McGoon DC, Murphy ML, Roe BB. A reporting system on subjects evaluated for coronary artery disease. Report of the Ad Hoc Committee for Grading of Coronary Artery Disease, Council on Cardiovascular Surgery, American Heart Association. Circulation 1975;51:55-40.
18. Leipsic J, Abbara S, Achenbach S, Cury R, Earls JP, Mancini GJ, Nieman K, Pontone G, Raff GL. SCCT guidelines for the interpretation and reporting of coronary CT angiography: a report of the Society of Cardiovascular Computed Tomography Guidelines Committee. J Cardiovasc Comput Tomogr 2014;8:342-58.
19. Rumberger JA, Brundage BH, Rader DJ, Kondos G. Electron beam computed tomographic coronary calcium scanning: a review and guidelines for use in asymptomatic persons. Mayo Clin Proc 1999;74:243-52.
20. Zinsser D, Marcus R, Othman AE, Bamberg F, Nikolaou K, Flohr T, Notohamiprodjo M. Dose Reduction and Dose Management in Computed Tomography - State of the Art. Rofo 2018;190:531-41.
21. Ding L, Chen M, Li X, Wu Y, Li J, Deng S, Xu Y, Chen Z, Yan C. Ultra-low dose dual-layer detector spectral CT for pulmonary nodule screening: image quality and diagnostic performance. Insights Imaging 2025;16:11.
22. Chu PW, Stewart C, Kofler C, Mahendra M, Wang Y, Chu CA, Lee C, Bolch WE, Smith-Bindman R. Representative Organ Doses from Computed Tomography (CT) Exams from a Large International Registry. Radiat Res 2025;203:1-9.
23. Golbus AE, Schuzer JL, Steveson C, Rollison SF, Matthews J, Henry-Ellis J, Razeto M, Chen MY. Reduced dose helical CT scout imaging on next generation wide volume CT system decreases scan length and overall radiation exposure. Eur J Radiol Open 2024;13:100578.
24. Wang J, Sui X, Zhao R, Du H, Wang J, Wang Y, Qin R,

Lu X, Ma Z, Xu Y, Jin Z, Song L, Song W. Value of deep learning reconstruction of chest low-dose CT for image quality improvement and lung parenchyma assessment on lung window. Eur Radiol 2024;34:1053-64.
25. Fitton I, Charpentier E, Arsovic E, Isaia J, Guillou M, Saltel-Fulero A, Fournier L, Van Ngoc Ty C. A Proposal for a Process from as Low as Reasonably Achievable to an Ultra-Low-Level Goal in Chest Computed Tomography. J Clin Med 2024;13:4597.
26. Dasegowda G, Mikhail Lette M, Achoki S, Affes M, Baichoo S, Karout L, et al. Multicenter, international study of CT practices and radiation doses from 10 African countries: An International Atomic Energy Agency (IAEA) baseline study. Phys Med 2024;124:103431.
27. Alenazi K. Radiation Doses in Routine CT Examinations for Adult Patients in Saudi Arabia: A Systematic Review. Cureus 2024;16:e64646.
28. Apfaltrer G, Albrecht MH, Schoepf UJ, Duguay TM, De Cecco CN, Nance JW, De Santis D, Apfaltrer P, Eid MH, Eason CD, Thompson ZM, Bauer MJ, Varga-Szemes A, Jacobs BE, Sorantin E, Tesche C. High-pitch low-voltage CT coronary artery calcium scoring with tin filtration: accuracy and radiation dose reduction. Eur Radiol 2018;28:3097-104.
29. Faure ME, Swart LE, Dijkshoorn ML, Bekkers JA, van Straten M, Nieman K, Parizel PM, Krestin GP, Budde RPJ. Advanced CT acquisition protocol with a third-generation dual-source CT scanner and iterative reconstruction technique for comprehensive prosthetic heart valve assessment. Eur Radiol 2018;28:2159-68.
30. Buchhave EØ, Rasmussen CD, Lentz R, Frederiksen EH, Kipp JO, Leftes MØ. Effect of arm position on image quality and radiation dose during thorax and abdomen computed tomography scans. Radiography (Lond) 2024;30:1035-40.
31. Franck C, Zhang G, Deak P, Zanca F. Preserving image texture while reducing radiation dose with a deep learning image reconstruction algorithm in chest CT: A phantom study. Phys Med 2021;81:86-93.
32. Jiang B, Li N, Shi X, Zhang S, Li J, de Bock GH, Vliegenthart R, Xie X. Deep Learning Reconstruction Shows Better Lung Nodule Detection for Ultra-Low-Dose Chest CT. Radiology 2022;303:202-12.
33. Kim JH, Yoon HJ, Lee E, Kim I, Cha YK, Bak SH. Validation of Deep-Learning Image Reconstruction for Low-Dose Chest Computed Tomography Scan: Emphasis on Image Quality and Noise. Korean J Radiol 2021;22:131-8.
34. Zhou Y, Hu L, Du S, Jin R, Li W, Lv F, Zhang Z. The ultrafast, high-pitch turbo FLASH mode of third-generation dual-source CT: Effect of different pitch and corresponding SFOV on image quality in a phantom study. J Appl Clin Med Phys 2021;22:158-67.
35. Flohr TG, Leng S, Yu L, Aiimendinger T, Bruder H, Petersilka M, Eusemann CD, Stierstorfer K, Schmidt B, McCollough CH. Dual-source spiral CT with pitch up to 3.2 and 75 ms temporal resolution: image reconstruction and assessment of image quality. Med Phys 2009;36:5641-53.
36. van Assen M, Martin SS, Varga-Szemes A, Rapaka S, Cimen S, Sharma P, Sahbaee P, De Cecco CN, Vliegenthart R, Leonard TJ, Burt JR, Schoepf UJ. Automatic coronary calcium scoring in chest CT using a deep neural network in direct comparison with non-contrast cardiac CT: A validation study. Eur J Radiol 2021;134:109428.
37. Eng D, Chute C, Khandwala N, Rajpurkar P, Long J, Shleifer S, et al. Automated coronary calcium scoring using deep learning with multicenter external validation. NPJ Digit Med 2021;4:88.
38. Jennings GL, Audehm R, Bishop W, Chow CK, Liaw ST, Liew D, Linton SM. National Heart Foundation of Australia: position statement on coronary artery calcium scoring for the primary prevention of cardiovascular disease in Australia. Med J Aust 2021;214:434-9.
39. Arnett DK, Blumenthal RS, Albert MA, Buroker AB, Goldberger ZD, Hahn EJ, Himmelfarb CD, Khera A, Lloyd-Jones D, McEvoy JW, Michos ED, Miedema MD, Muñoz D, Smith SC Jr, Virani SS, Williams KA Sr, Yeboah J, Ziaeian B. 2019 ACC/AHA Guideline on the Primary Prevention of Cardiovascular Disease: A Report of the American College of Cardiology/American Heart Association Task Force on Clinical Practice Guidelines. Circulation 2019;140:e596-646.

Cite this article as: Shu YL, Yu H, Guo DJ, Huang YP, Jiang WL, Luo YD, Xu J. Comparison of chest computed tomography in Turbo FLASH mode with conventional mode for coronary artery disease screening: radiation dose, image quality, and calcium scoring performance. Quant Imaging Med Surg 2025;15(3):2420-2432. doi: 10.21037/qims-24-1005

